

COGNAC

Circuit Optimization via Gradients and Noise-Aware Compilation

Finn Voichick

University of Maryland
College Park, United States
finn@umd.edu

Leonidas Lampropoulos

University of Maryland
College Park, United States
leonidas@umd.edu

Robert Rand

University of Chicago
United States
rand@uchicago.edu

Abstract

We present COGNAC, a novel strategy for compiling quantum circuits based on numerical optimization algorithms from scientific computing. Using a simple noise model informed by the duration of entangling gates, our gradient-based method can quickly converge to a local optimum that closely approximates the target unitary. By iteratively and continuously decreasing a gate’s duration to zero, we reduce a circuit’s gate count without the need for a large number of explicit elimination rewrite rules. We have implemented this technique as a general-purpose Qiskit compiler plugin and compared performance with state-of-the-art optimizers on a variety of standard 4-qubit benchmarks. COGNAC typically outperforms existing optimizers in reducing 2-qubit gate count, sometimes significantly. Running on a low-end laptop, our plugin takes seconds to optimize a small circuit, making it effective and accessible for a typical quantum programmer.

1 Introduction

Compiling a quantum program can involve a number of intermediate representations, but generally entails the construction of a quantum circuit, a sequence of quantum logic gates at an abstraction level comparable to assembly languages in classical computing [2, 6]. Quantum circuit optimizers, like their classical counterparts, employ rewrite rules to shorten these circuits, and recent research in this area has seen impressive developments, both in the number of such equivalences and the strategies for applying them [11, 24]. While this basic *rewriting* scheme is sensible and familiar to computer scientists, it differs significantly from the *numerical* optimizations that physicists perform on the same quantum systems.

Quantum hardware specialists work at a lower level of abstraction, dealing directly with hardware channels in the language of microwave pulses. Indeed, quantum optimal control theory has progressed significantly in recent years, manipulating pulse schedules and implementing the gates that quantum programmers take for granted [8]. Optimization at this level must acknowledge two key features of quantum systems that logic gates tend to abstract away: control is both *noisy* and *continuous*.

Noise is a defining characteristic of the noisy intermediate-scale quantum era (NISQ), which describes the current state

$$\begin{aligned}
 R_x(\theta) &:= \begin{bmatrix} \cos(\theta/2) & -i \sin(\theta/2) \\ -i \sin(\theta/2) & \cos(\theta/2) \end{bmatrix} \\
 R_y(\theta) &:= \begin{bmatrix} \cos(\theta/2) & -\sin(\theta/2) \\ \sin(\theta/2) & \cos(\theta/2) \end{bmatrix} \\
 R_z(\theta) &:= \begin{bmatrix} e^{-i\theta/2} & 0 \\ 0 & e^{i\theta/2} \end{bmatrix} \\
 R_{zz}(\theta) &:= \begin{bmatrix} e^{-i\theta/2} & 0 & 0 & 0 \\ 0 & e^{i\theta/2} & 0 & 0 \\ 0 & 0 & e^{i\theta/2} & 0 \\ 0 & 0 & 0 & e^{-i\theta/2} \end{bmatrix}
 \end{aligned}$$

Figure 1. A parameterized gate set

of quantum computing [16]. Precisely modeling atomic interactions is notoriously difficult, and unintended side effects are non-negligible. Optimal pulse engineering is a matter of *minimizing* (not *eliminating*) this noise, and the computational tools brought to bear in solving this optimization problem differ significantly from those employed in traditional compilers. The control parameters at this level are real-valued and continuous, meaning that any pulse-level instruction can be divided and subdivided (for example, by halving the amplitude in a microwave pulse schedule). This procedure has become a time-consuming, specialized, and iterative one, involving physical modeling, calculus, and experimentation. It is no wonder, then, that optimizers shy away from this domain, reinforcing the quantum logic gate as a standard abstraction barrier between analog pulse optimization and digital compiler optimization, with physicists on one side and computer scientists on the other.

Recent work has just begun to blur this boundary between analog and digital compilation. Compilers have been making better use of real-parameterized gates like the one in Figure 1, which is partly responsible for the current records in quantum volume performance benchmarks [17]. Quantum devices can implement these gates by continuously adjusting the real parameters of a pulse envelope [5]. General-purpose quantum circuit compilers like Qiskit [22] and TKET [19] now allow users to specify the estimated fidelity (accuracy) of the hardware’s native two-qubit gates, information that is used for approximations when synthesizing general two-qubit gates. These compilers can then produce a smaller

compiled circuit that is not logically equivalent to the original, but whose output distribution suffers from less noise and thus ends up implementing the idealized original circuit more faithfully than the (noisy) original circuit itself.

We propose to further blur the line between pulse-level (analog) and gate-level (digital) quantum computing, enhancing compilers with not only continuous control and noise awareness, but also iterative calculus-informed optimization techniques. Algorithms for optimizing continuous, differentiable functions are already well-developed, and exposing these lower level mechanisms to higher level compilation passes allows for more flexible optimizations.

In their current state, these strategies typically involve an iterative process with significant computation and experiments on hardware, so adapting it to the setting of compiler optimizations requires some changes. The most significant change in our experiments has been a major simplification to the noise model of the quantum system. Rather than precisely modeling the complex interactions that occur within quantum hardware and trying to characterize different types of noise (leakage into higher energy states, T1/T2 decoherence, cross-talk, etc.), we rely on a simplifying assumption: *shorter pulses produce smaller errors*. While not as accurate as the noise models typically employed in quantum optimal control, experiments have found it to be a valid approximation in practice [14]. More importantly, it leads to an efficiently differentiable cost function that encourages zero-duration pulses, which can then be eliminated from the circuit. We thus find a reasonable middle ground between large-scale circuit optimization and experimentally-driven pulse engineering, decreasing gate count in an iterative, gradient-driven way at a moderate scale without the need for additional hardware calibrations.

To bridge this division between pulse optimization and compilers, we developed COGNAC: Circuit Optimization via Gradients and Noise-Aware Compilation. In the following sections, we detail our strategy and its implementation as a Qiskit compiler plugin, and we then evaluate and compare its performance relative to existing optimizers. We hope that our technique serves as a useful tool for improving performance on near-term quantum hardware.

Contributions. This paper presents COGNAC, a general-purpose noise-aware quantum circuit optimizer adapted from lower-level pulse optimization strategies. Using gradient-based numerical optimization to eliminate two-qubit gates, our implementation of COGNAC outperforms state-of-the-art optimizers on most of the four-qubit benchmarks tested. COGNAC typically requires seconds to run on these circuits without substantially reducing the accuracy of the resulting circuit, either in theory or in practice.

2 Technique

COGNAC is most effective with circuits consisting largely of parameterized rotation gates, such as the one in Figure 2, a small quantum Fourier transform circuit taken from MQT Bench [18]. In this circuit, all the two-qubit gates are R_{zz} gates, and we represent parameterized R_z gates with a single black circle. Given such a circuit, we fix its general gate structure (or *ansatz*) and consider the effect of changing the parameter values alone, as in Figure 3. All of the parameters $\theta_1, \dots, \theta_n$ can be viewed as a single vector $\vec{\theta} \in \mathbb{R}^n$ (where $n = 23$ in this case). The ansatz defines a matrix-valued function $U(\vec{\theta})$ describing the ideal unitary implemented by the circuit with those parameter values.¹ If the input parameters are $\vec{\theta}_0$, then there will in general be other possible settings $\vec{\theta}_\star$ such that $U(\vec{\theta}_\star) \approx U(\vec{\theta}_0)$. Such alternative parameters still approximate the target unitary and may be preferable to $\vec{\theta}_0$. For example, note that an $R_{zz}(0)$ gate is an identity operator, so decreasing one of the parameters to 0 means the elimination of a (costly) two-qubit gate.

To express these preferences, we can devise a *figure of merit* to be used with gradient ascent. (This is the opposite of a *cost function* used for gradient descent, an equivalent way to frame the problem.) The standard figure of merit for pulse engineering [12] would be $|\text{trace}(U(\vec{\theta}_0)^\dagger U'(\vec{\theta}_\star))|$, assuming that $U'(\cdot)$ accounts for noise.

For the sake of simplicity, we model the noise with

$$U'(\vec{\theta}_\star) = \mathcal{F}(\vec{\theta}_\star)U(\vec{\theta}_\star).$$

Here, $\mathcal{F} : \mathbb{R}^n \rightarrow [0, 1]$ is a differentiable fidelity function that we will define more precisely in Section 3.1. For now, just note that it decays approximately exponentially with the sum of all the two-qubit rotation angles θ . This model – effectively depolarizing noise proportional to the size of the circuit² – is simpler and less precise than the noise models typically used in pulse engineering, but it has the advantage that it is fast to compute and differentiate while still general enough to be useful on a variety of quantum hardware.

An existing gradient-based optimization algorithm (in our case L-BFGS-B [26]) can then adjust the parameters to maximize the figure of merit, using the gradient to inform its search direction. In this example, the optimizer converges to a local optimum where both θ_{11} and θ_{14} are set to zero. A subsequent compiler pass can eliminate these two gates from the circuit, reducing the two-qubit gate count from five to three. This particular example is small enough that existing optimizers could optimally synthesize the entire two-qubit

¹We assume that the input circuit is sufficiently small that this function U can be evaluated efficiently. In practice, this technique applies to moderately sliding windows (say, four or five qubits) and serves as a peephole optimization.

²A depolarizing noise model assumes that the quantum state decays into a maximally mixed state with probability $1 - \mathcal{F}(\vec{\theta}_\star)$, which increases with the duration of the circuit’s entangling gates.

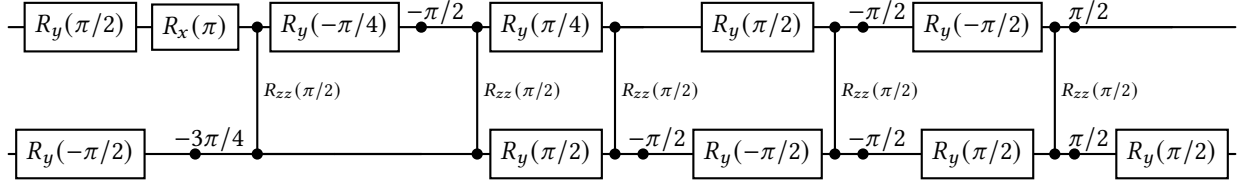


Figure 2. An example input circuit

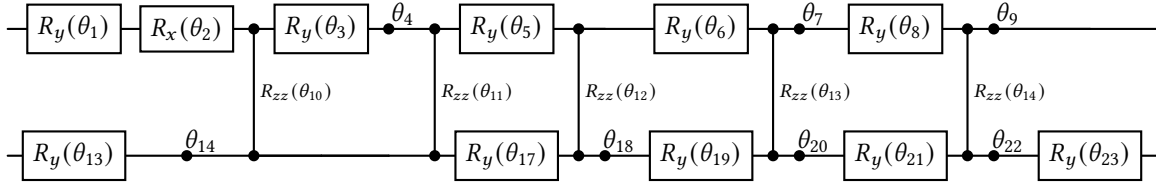
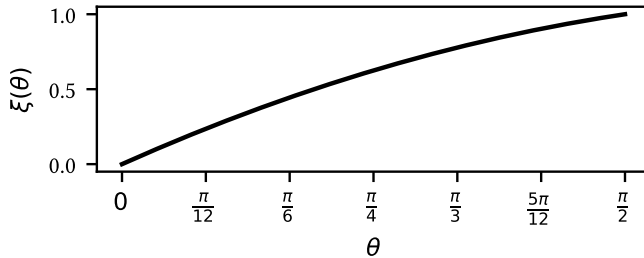


Figure 3. The ansatz derived from the input circuit


 Figure 4. The error function ξ

circuit, but COGNAC has the advantage of being far more general: it readily applies to larger circuits without changing the gate set or connectivity constraints.

3 Implementation

We have implemented COGNAC as an open-source Qiskit compiler plugin [21]. It divides an arbitrary input circuit into (possibly overlapping) maximal four-qubit windows, and then relies on SciPy’s implementation of the L-BFGS-B quasi-Newton optimization algorithm [20, 26]. Most of the interesting implementation work is thus in constructing an efficient cost function (or figure of merit) and its gradient. To validate our circuits on IBM’s superconducting machines, we used pulse-level control to extend their gate set to the one in Figure 1. We will discuss each of these developments in more detail.

3.1 Figure of Merit

COGNAC is designed to run relatively late in the compilation process, after gates have been decomposed into a native gate set and logical qubits have been mapped to the hardware layout. COGNAC then optimizes a four-qubit subcircuit in which all two-qubit gates are parameterized.

As mentioned earlier, we use a standard figure of merit, $|\text{trace}(U(\vec{\theta}_0)^\dagger U'(\vec{\theta}_\star))|$, assuming U is an idealized unitary for the target operator and U' approximates noise. Each of these is calculated as the product of a series of matrices, each corresponding to a gate in the circuit. With U , these matrices are those from Figure 1, but for U' , we account for noisy R_{zz} (or equivalent) gates using the model:

$$R'_{zz}(\theta) := (1 - E \cdot \xi(\theta))R_{zz}(\theta)$$

$$\xi(\theta) := \theta(3\pi - 2\theta)/\pi^2$$

Here, E is a hardware-dependent constant describing the benchmarked two-qubit error rate, for example 0.01 when targeting a system with 99% fidelity R_{zz} gates. The function ξ , depicted in Figure 4, describes how the error scales with the angle of rotation. This definition ensures that $\xi(\pi/2) = 1$ and $\xi(0) = 0$ (accounting for the presence or absence of a fully entangling gate), and its positive derivative encourages the optimizer to follow the gradient to a zero-duration gate. Aside from those specifications, our ξ is somewhat arbitrary. Picking $\xi(\theta) = 2\theta/\pi$ or $\xi(\theta) = \sin^2 \theta$ would have been just as valid and may model certain hardware more accurately. In practice, we find that these functions lead to circuits with a large number of small-angle gates, and by making the gradient steeper around $\theta \approx 0$, we encourage more of these angles to drop to $\theta = 0$.

The function $U(\cdot)$ is a linear function of the sines and cosines of the various rotation angles, and the noise model adds a quadratic multiplier, so computing the gradient of our figure of merit is relatively straightforward. We implement all of this calculation using NumPy’s libraries for matrix multiplication, and SciPy evaluates the gradient many times as it searches for better parameters.

One side effect of tracking the error on a per-gate basis is that it becomes possible to use different values of E for the different hardware gates. On systems that report the

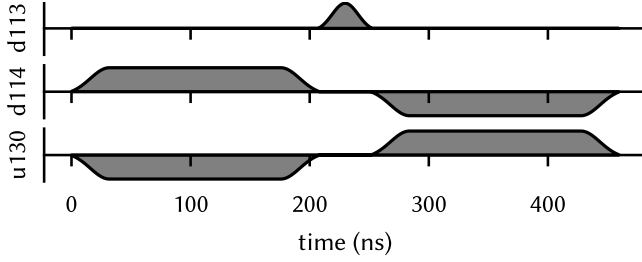


Figure 5. IBM’s calibrated pulse schedule for an eCR gate

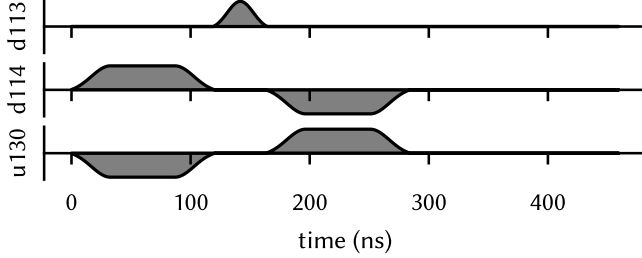


Figure 6. Our pulse schedule for an $\text{feCR}(\pi/4)$ gate

fidelities of their individual two-qubit gates, this allows us to encourage the optimizer to prioritize shortening those gates which are especially noisy, in effect doing more computation on the higher-fidelity qubits.

3.2 Pulse squishing

Many quantum hardware providers include parameterized two-qubit gates in their native gate sets; for example, Quantinuum machines include an R_{zz} gate, IonQ has an R_{xx} gate, and Rigetti has a parameterized $i\text{SWAP}$ gate. IBM’s machines do not include such gates, but they *do* allow for pulse-level control of their hardware. To demonstrate COGNAC’s applicability to these systems, we have used IBM’s pulse-level control to implement our own arbitrary-angle entangling gates. Our feCR (fractional echo-cross-resonance) gate is a generalization of the standard eCR = feCR($\pi/2$) gate:

$$\text{feCR}(\theta) := \begin{bmatrix} 0 & 0 & i \cos \frac{\theta}{2} & -\sin \frac{\theta}{2} \\ 0 & 0 & -\sin \frac{\theta}{2} & i \cos \frac{\theta}{2} \\ i \cos \frac{\theta}{2} & \sin \frac{\theta}{2} & 0 & 0 \\ \sin \frac{\theta}{2} & i \cos \frac{\theta}{2} & 0 & 0 \end{bmatrix}$$

Implementing high-fidelity gates is normally an involved process that requires numerous experiments and regular recalibrations. To avoid this complication, we bootstrap our pulse schedules from existing calibrations. IBM regularly calibrates the pulse schedule for their echo-cross-resonance (eCR) gates, and Figure 5 depicts the pulse envelopes for an eCR gate between qubits 113 and 114 on IBM’s Cusco machine.

The eCR (echo-cross-resonance) gate is essentially two R_{zx} opposing interactions sandwiching a standard Pauli- X

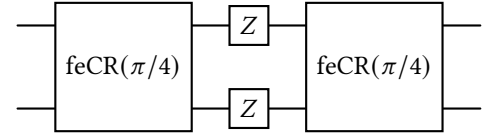


Figure 7. A Clifford gate construction for benchmarking

gate [9]. This is visible in Figure 5, where channel d113 enacts the X gate, channel u130 is the coupler implementing the R_{zx} interactions, and channel d114 is calibrated to cancel out unwanted side effects of the coupler. By “squishing” the pulse envelopes for the R_{zx} segments, we can decrease the R_{zx} rotation angles. The interaction strength is approximately proportional to the area under the curve, so Figure 6 depicts an feCR($\pi/4$) pulse schedule based on the standard eCR($\pi/2$) schedule.

This “bootstrapping” process is similar to previous work that adjusts the *amplitude* of pre-calibrated pulses [5]. Dilating the *time* axis has the additional benefit of a shorter runtime, potentially leading to improved coherence. We keep the pulse frequency, amplitude, and rise/fall shape from IBM’s existing calibrations.

Experimental validation. Preliminary experiments run on IBM’s machines show that our feCR gates have reasonably high fidelity in practice. We performed a small interleaved randomized benchmarking experiment comparing IBM’s eCR gate to our feCR($\pi/4$) gate. Because interleaved randomized benchmarking is restricted to Clifford gates [13], we constructed one from two feCR($\pi/4$) gates, as shown in Figure 7. (The Z gates are *virtual* gates with negligible error rates, included so that the resulting Clifford gate is nontrivial, as the feCR gate is self-adjoint.) This is similar in principle to previous work benchmarking a small-angle R_{xx} gate by concatenating it many times [14]. Though the eCR gate is a Clifford gate, we test it using the same concatenated structure to ensure a fair comparison, replacing the feCR($\pi/4$) gates in Figure 4 with eCR gates.

We tested the resulting Cliffords on qubits 113 and 114 of IBM’s Cusco machine. We find that the eCR pair has an error rate of 0.0172 ± 0.0019 , and the feCR($\pi/4$) pair has an error rate of 0.0112 ± 0.0012 . Further testing is needed to generalize these findings, but these results suggest that our fractional-angle entangling gates perform better than their maximally-entangling counterparts.

4 Evaluation

To evaluate COGNAC, we compare its performance on benchmark circuits with that of three existing quantum circuit optimizers: Qiskit [22], TKET [19], and Queso [24]. On most of the benchmarks, COGNAC produces fewer two-qubit gates than any of the other optimizers, and its output circuits still approximate the input circuits with reasonably high fidelity.

COGNAC’s runtime is consistently the second-longest (after Queso), but it is usually a matter of seconds for these four-qubit circuits. Queso’s runtime is effectively bounded only by the user’s set time limit, and we limit it to five minutes, far longer than any of the other optimizers take.

Benchmarks. We use all the four-qubit benchmark circuits from MQT Bench [18]. To limit the scope to post-routing optimization, we use the versions of the circuits that have already been mapped (via TKET) to the IBM Montreal hardware layout, and we configure all of the optimizers to preserve qubit layout, disallowing “virtual SWAP” gates. Because of this mapping process, our input circuits have already been partially optimized, and the tested optimizers are often unable to find any way to reduce two-qubit gate count.

Four qubits is rather small, and COGNAC has a distinct advantage at this scale because it can optimize the entire circuit at once. We use this size in part because it is supported by almost all the variable-size MQT benchmarks, and it allows us to pick a standard canonical circuit size for the tables rather than aggregating data from the hundreds of MQT benchmarks of various sizes. A smaller circuit size also makes it possible to simulate the output circuit classically and measure the idealized fidelity of the circuit as a whole. COGNAC supports circuits of arbitrary size, but larger circuits are divided into smaller optimization windows to avoid exponentially large matrix multiplications.

4.1 Circuit metrics

Gate count. We ran all of our benchmark circuits through the different optimizers and recorded the size of the output circuits. We measure performance using two-qubit gate count, as these are the main source of error on near-term devices (e.g. IBM’s Eagle r3 devices [7]). Different compilers sometimes perform better with different gate sets, and we tried to run each optimizer using its preferred gate set. TKET uses the R_{zz} gate, and COGNAC uses our feCR gate, which are equivalent given additional single-qubit gates. Qiskit and Queso primarily use the CNOT gate, which can be implemented with one $R_{zz}(\pi/2)$ gate, so the two-qubit gate counts are directly comparable.

Table 1 lists the results from our tests, with the lowest gate count for each benchmark bolded (whenever there is only one). COGNAC usually performs better than all the others. Sometimes this improvement is significant, for example in the circuit `qwalk-noancilla`, where COGNAC’s two-qubit gate count is less than 1/5th the count of the other optimizers. Some of the circuits, such as `ghz`, cannot be improved by any optimizer, including COGNAC.

We include a similar table for two-qubit circuit *depth* in Appendix A.

Fidelity. Queso employs only *exact* rewrites that lead to semantically equivalent circuits, and Qiskit and TKET

also behave this way by default. However, this requirement of perfection is too restrictive in practice because modern hardware is noisy and *no* rewrite is truly perfect in practice. Qiskit and TKET (like COGNAC) therefore allow the user to input the estimated fidelity of their native two-qubit gates. This information is used during two-qubit gate synthesis to eliminate some small-angle rotations, producing circuits that are not strictly equivalent to the inputs but expected to be more accurate. For all of these benchmarks, we tell the optimizers that fully entangling two-qubit gates have 99% fidelity. In Appendix B, we include additional data collected under assumptions of 98% and 99.9%.

The parenthesized fidelities listed in Table 1 represent the *idealized* fidelity of the output circuit compared to the original input. COGNAC makes heavy use of approximations, leading to output circuits that are not mathematically equivalent to their inputs but closely approximate them. Because Queso produces mathematically equivalent circuits, its idealized fidelities are always 100%. Qiskit and TKET sometimes take advantage of gate-count-reducing approximations, but only at the scale of two qubit subcircuits, so they are more conservative in general than COGNAC.

Measuring the *actual* fidelity of these circuits is a challenging task. There are efficient ways to benchmark certain classes of circuits; for example, interleaved randomized benchmarking assesses Clifford gates. These benchmarks, however, cover a diverse range of problems [18]. In general, precisely characterizing a quantum channel’s fidelity requires a number of physical experiments exponential in the number of qubits [4], which quickly becomes prohibitive. As a result, comparisons of quantum circuit optimizers tend to involve fidelity estimates based on classically-computed circuit metrics [11, 24]. Under the assumption that all two-qubit gates have 99% fidelity and single-qubit gate errors are negligible, we approximate the process fidelity as $F \cdot 0.99^n$, where F is the idealized process fidelity from Table 1 and n is the number of two-qubit gates. (This neglects the fact that shorter-duration gates tend to have higher fidelity [14].) Table 2 lists these calculations for the various optimizers, with differences of more than ten percentage points bolded. Though these numbers are only rough estimates of practical performance, they show that COGNAC’s decreased gate counts generally make up for its approximations.

4.2 Compile time

We tested all the optimizers on a standard consumer laptop.³ Table 3 shows the median optimization time over five different runs. Queso is designed to continue searching for optimizations until it reaches a timeout, so we limited it to five minutes, significantly more than any of the others used.

³A 2021 Asus ZenBook with an Intel Core i7 processor, 16GB RAM, and no dedicated graphics card

Table 1. Two-qubit output metrics from various optimizers

Benchmark	Optimized gate count (idealized fidelity where applicable)				
	Unoptimized	Qiskit	TKET	Queso	COGNAC
ae	16	16 (100%)	11 (100%)	16	12 (99.9%)
dj	3	3 (100%)	3 (100%)	3	3 (100%)
ghz	3	3 (100%)	3 (100%)	3	3 (100%)
graphstate	8	8 (100%)	8 (100%)	8	8 (100%)
groundstate	20	20 (100%)	19 (100%)	20	17 (99.8%)
grover-noancilla	69	69 (100%)	52 (100%)	69	24 (96.8%)
grover-v-chain	69	69 (100%)	52 (100%)	69	24 (96.8%)
portfolioqaoa	52	52 (100%)	35 (100%)	52	27 (97.0%)
portfoliovqe	34	34 (100%)	32 (100%)	34	22 (98.9%)
qaoa	22	18 (100%)	14 (100%)	22	15 (98.7%)
qft	18	16 (99.0%)	11 (99.0%)	18	14 (98.7%)
qftentangled	19	17 (99.0%)	13 (99.0%)	19	10 (99.8%)
qnn	40	21 (86.1%)	30 (99.8%)	40	25 (91.6%)
qpeexact	8	8 (100%)	6 (100%)	8	7 (99.9%)
qpeinexact	14	13 (99.0%)	10 (100%)	14	14 (98.9%)
qwalk-noancilla	163	163 (100%)	157 (100%)	163	30 (99.6%)
random	37	36 (99.1%)	32 (100%)	37	30 (99.1%)
realamprandom	34	34 (100%)	32 (100%)	34	27 (97.6%)
su2random	34	34 (100%)	32 (100%)	34	23 (98.1%)
tsp	15	15 (100%)	15 (100%)	15	8 (97.2%)
twolocalrandom	34	34 (100%)	32 (100%)	34	27 (97.6%)
vqe	6	6 (100%)	6 (100%)	6	6 (100%)
wstate	6	6 (100%)	6 (100%)	6	6 (99.9%)

In most cases, it used the full 300 seconds. The one exception was the ghz benchmark, which is sufficiently small that Queso was able to exhaust all possibilities and terminate early.

COGNAC is time-consuming relative to the other optimizers, but the runtimes are short enough that it could be integrated into a general-purpose compiler toolchain. The circuit that was the most optimized, qwalk-noancilla, was also the most time-consuming by far.

COGNAC divides larger circuits into four-qubit sliding windows, and so we expect its runtime to grow linearly with the input circuit’s gate count. Its execution is currently single-threaded, but it could easily be adapted to optimize non-overlapping windows in parallel. Unlike most optimizers, COGNAC could run significantly faster if re-implemented for GPUs, which have already accelerated the L-BFGS-B algorithm [3] and other aspects of quantum control [10] by more than an order of magnitude.

5 Discussion

Quantum compilers are an active area of research, and they draw heavily on ideas from classical compilers. This influence has benefitted quantum programmers, but the resulting

compiler optimizations tend to be discrete and exact rewrites, even though quantum control is continuous and noisy in practice. In this work, we have shown that continuous approximate optimization can be useful too, and that the boundaries between pulse engineering and compiler optimization need not be so rigid.

This paper focuses on a modification of one of IBM’s gate sets, but our strategy should readily apply to others as well. COGNAC works with several different gate sets, and could easily be extended further.⁴ We hope that COGNAC can become a standard tool in a typical quantum development workflow, one from which quantum programmers can benefit without an understanding of its inner workings.

5.1 Prior work

COGNAC attempts to blur the line between compiler optimization and pulse engineering, and developments from both of these research areas have influenced its principles.

Gate-level optimizers, like optimizers for classical programs, tend to rely on rewriting rules. A notable exception is

⁴It is worth noting that our informal tests found that COGNAC was less helpful on architectures with all-to-all connectivity where virtual SWAP gates avoid some of the overhead that COGNAC helps to optimize away.

Table 2. Estimated fidelity from various optimizers

Benchmark	Estimated optimized fidelity			
	Qiskit	TKET	Queso	COGNAC
ae	85%	90%	85%	89%
dj	97%	97%	97%	97%
ghz	97%	97%	97%	97%
graphstate	92%	92%	92%	92%
groundstate	82%	83%	82%	84%
grover-noancilla	50%	59%	50%	76%
grover-v-chain	50%	59%	50%	76%
portfolioqaoa	59%	70%	59%	74%
portfoliovqe	71%	72%	71%	79%
qaoa	83%	87%	80%	85%
qft	84%	89%	83%	87%
qftentangled	83%	87%	83%	90%
qnn	70%	74%	67%	71%
qpeexact	92%	94%	92%	93%
qpeinexact	87%	90%	87%	86%
qwalk-noancilla	19%	21%	19%	74%
random	69%	72%	69%	73%
realamprandom	71%	72%	71%	74%
su2random	71%	72%	71%	78%
tsp	86%	86%	86%	90%
twolocalrandom	71%	72%	71%	74%
vqe	94%	94%	94%	94%
wstate	94%	94%	94%	94%

in the synthesis of two-qubit gates, for which a general procedure exists that is known to be optimal [1]. TKET applies this procedure to every two-qubit gate in a circuit, reducing the number of consecutive gates applied to the same two qubits [19]. This synthesis has been improved by accounting for noise and including fractional-angle gates, but it is still limited to two-qubit gates.

Some researchers have noted that there are a number of different gate sets for different quantum hardware and that rewrite rules necessarily make assumptions about gate sets that may not apply. One solution to this problem has been the automatic generation of large numbers of rewrite rules for an arbitrary gate set, as done by Quartz [25] and Queso [24]. Quartz is notable for its guarantee of generating *all* possible rewrite rules of a given size, but requires considerable computational resources. Queso represents gate parameters as symbolic angles, allowing them to generate rewrite rules like “ $R_z(\alpha)R_z(\beta) \mapsto R_z(\alpha+\beta)$.” However, the symbolic transformations are limited to relatively simple formulas like this one, and both of these systems are limited to *exact* rewrites.

Quarl [11] is another recent quantum circuit optimizer that builds on Quartz’s generated rewrite rules, but uses reinforcement learning on a neural network to decide which

Table 3. Compile time of various optimizers

Benchmark	Optimization time (s)			
	Qiskit	TKET	Queso	COGNAC
ae	0.1	0.2	>300	0.9
dj	<0.1	0.1	>300	0.1
ghz	<0.1	<0.1	2	0.1
graphstate	<0.1	0.1	>300	0.1
groundstate	0.1	0.3	>300	2.0
grover-noancilla	0.1	0.8	>300	37.2
grover-v-chain	0.1	0.8	>300	36.9
portfolioqaoa	0.1	0.5	>300	10.7
portfoliovqe	0.1	0.4	>300	4.7
qaoa	0.1	0.2	>300	2.1
qft	0.1	0.2	>300	3.1
qftentangled	0.1	0.2	>300	2.7
qnn	0.3	0.4	>300	7.6
qpeexact	<0.1	0.1	>300	0.7
qpeinexact	0.1	0.2	>300	0.5
qwalk-noancilla	0.2	1.9	>300	76.5
random	0.1	0.4	>300	5.8
realamprandom	0.1	0.4	>300	1.5
su2random	0.1	0.4	>300	5.4
tsp	0.1	0.2	>300	1.3
twolocalrandom	0.1	0.4	>300	1.6
vqe	<0.1	0.1	>300	0.1
wstate	<0.1	0.1	>300	0.3

rewrites to perform. Unfortunately, it is designed to run for hours on a supercomputer, so it is impractical as part of a typical compiler toolchain. Like Queso and Quartz, Quarl is limited to idealized equivalences and does not allow for approximations.

In the quantum control community, GRAPE (gradient ascent pulse engineering) has emerged as a popular tool for designing high-fidelity pulse sequences [8]. However, GRAPE’s pulses are only as accurate as its physical model of the quantum system, and noise can be difficult to precisely characterize on practical hardware [27]. Practical applications of GRAPE to produce well-calibrated gates tend to involve an iterative protocol involving feedback from hardware experiments [15, 23], making it unsuitable as part of a general-purpose compiler optimization. COGNAC fittingly aims to distill GRAPE’s key features while porting it to a different context.

5.2 Future work

In blurring the line between analog and digital quantum computing, we have exposed lower-level techniques to the

compiler, but future developments could expose further connections between these two levels of abstraction. If data-driven pulse engineering leads to more automated calibration of larger-scale circuit operations, then it could expose more hardware-specific information to future compilers. For example, there could be gate sets with three-qubit gates and more empirical noise models, which would require a more involved compiler.

COGNAC also has some limitations that future work could try to handle. An obvious one is the fixed input ansatz; COGNAC does not allow for gates to be reordered or applied to different qubits. Future optimizers could involve additional compilation passes designed to complement COGNAC by reordering gates or adding new ones. Quarl-style reinforcement learning could be useful here and for improving other elements of COGNAC, like its cost function and its process for selecting optimization windows in larger circuits.

As an open question, we wonder if there are domains outside of quantum computing where compilers would benefit from gradient-based optimization. There may be other applications where programs are typically framed in a discrete language, but a more continuous and approximate perspective could be beneficial.

Acknowledgments

This research used resources of the Oak Ridge Leadership Computing Facility, which is a DOE Office of Science User Facility supported under Contract DE-AC05-00OR22725. This material is supported by the Air Force Office of Scientific Research under award number FA95502310406. We thank Murphy Yuezhen Niu, Michael Hicks, and Benjamin Quiring for their useful feedback on an earlier draft of this report.

References

- [1] M Blaauboer and R L de Visser. An analytical decomposition protocol for optimal implementation of two-qubit entangling gates. *Journal of Physics A: Mathematical and Theoretical*, 41(39):395307, September 2008. [arXiv:cond-mat/0609750](#), doi:10.1088/1751-8113/41/39/395307.
- [2] Andrew W. Cross, Lev S. Bishop, John A. Smolin, and Jay M. Gambetta. Open quantum assembly language, 2017. [arXiv:1707.03429](#).
- [3] Yun Fei, Guodong Rong, Bin Wang, and Wenping Wang. Parallel L-BFGS-B algorithm on GPU. *Computers & Graphics*, 40:1–9, 2014. doi:10.1016/j.cag.2014.01.002.
- [4] Steven T. Flammia and Yi-Kai Liu. Direct fidelity estimation from few pauli measurements. *Phys. Rev. Lett.*, 106:230501, June 2011. [arXiv:1104.4695](#), doi:10.1103/PhysRevLett.106.230501.
- [5] Pranav Gokhale, Ali Javadi-Abhari, Nathan Earnest, Yunong Shi, and Frederic T. Chong. Optimized quantum compilation for near-term algorithms with OpenPulse. In *53rd Annual IEEE/ACM International Symposium on Microarchitecture*, pages 186–200, New York, 2020. IEEE. [arXiv:2004.11205](#), doi:10.1109/MICRO50266.2020.00027.
- [6] Keshu Hietala, Robert Rand, Shih-Han Hung, Xiaodi Wu, and Michael Hicks. A verified optimizer for quantum circuits. *Proc. ACM Program. Lang.*, 5(POPL), January 2021. [arXiv:1912.02250](#), doi:10.1145/3434318.
- [7] IBM. IBM Brisbane, 2024. URL: https://quantum.ibm.com/services/resources?system=ibm_brisbane.
- [8] Christiane P. Koch, Ugo Boscain, Tommaso Calarco, Gunther Dirr, Stefan Filipp, Steffen J. Glaser, Ronnie Kosloff, Simone Montangero, Thomas Schulte-Herbrüggen, Dominique Sugny, and Frank K. Wilhelm. Quantum optimal control in quantum technologies: Strategic report on current status, visions and goals for research in Europe. *EPJ Quantum Technology*, 9(1), July 2022. [arXiv:2205.12110](#), doi:10.1140/epjqt/s40507-022-00138-x.
- [9] P. Krantz, M. Kjaergaard, F. Yan, T. P. Orlando, S. Gustavsson, and W. D. Oliver. A quantum engineer’s guide to superconducting qubits. *Applied Physics Reviews*, 6(2):021318, June 2019. [arXiv:1904.06560](#), doi:10.1063/1.5089550.
- [10] Nelson Leung, Mohamed Abdelhafez, Jens Koch, and David Schuster. Speedup for quantum optimal control from automatic differentiation based on graphics processing units. *Phys. Rev. A*, 95:042318, Apr 2017. [arXiv:1612.04929](#), doi:10.1103/PhysRevA.95.042318.
- [11] Zikun Li, Jinjun Peng, Yixuan Mei, Sina Lin, Yi Wu, Oded Padon, and Zhihao Jia. Quarl: A learning-based quantum circuit optimizer, 2023. [arXiv:2307.10120](#).
- [12] S. Machnes, U. Sander, S. J. Glaser, P. de Fouquières, A. Gruslys, S. Schirmer, and T. Schulte-Herbrüggen. Comparing, optimizing, and benchmarking quantum-control algorithms in a unifying programming framework. *Phys. Rev. A*, 84:022305, August 2011. [arXiv:1011.4874](#), doi:10.1103/PhysRevA.84.022305.
- [13] Easwar Magesan, Jay M. Gambetta, B. R. Johnson, Colm A. Ryan, Jerry M. Chow, Seth T. Merkel, Marcus P. da Silva, George A. Keefe, Mary B. Rothwell, Thomas A. Ohki, Mark B. Ketchen, and M. Steffen. Efficient measurement of quantum gate error by interleaved randomized benchmarking. *Phys. Rev. Lett.*, 109:080505, August 2012. doi:10.1103/PhysRevLett.109.080505.
- [14] Yunseong Nam, Jwo-Sy Chen, Neal C. Panti, Kenneth Wright, Conor Delaney, Dmitri Maslov, Kenneth R. Brown, Stewart Allen, Jason M. Amini, Joel Apisdorf, Kristin M. Beck, Aleksey Blinov, Vandiver Chaplin, Mika Chmielewski, Coleman Collins, Shantanu Debnath, Kai M. Hudek, Andrew M. DuCore, Matthew Keesan, Sarah M. Kreikemeier, Jonathan Mizrahi, Phil Solomon, Mike Williams, Jaime David Wong-Campos, David Moehring, Christopher Monroe, and Jungsang Kim. Ground-state energy estimation of the water molecule on a trapped-ion quantum computer. *npj Quantum Information*, 6(1):33, April 2020. [arXiv:1902.10171](#), doi:10.1038/s41534-020-0259-3.
- [15] Riccardo Porotti, Vittorio Peano, and Florian Marquardt. Gradient-ascent pulse engineering with feedback. *PRX Quantum*, 4:030305, Jul 2023. [arXiv:2203.04271](#), doi:10.1103/PRXQuantum.4.030305.
- [16] John Preskill. Quantum computing in the NISQ era and beyond. *Quantum*, 2:79, August 2018. [arXiv:1801.00862](#), doi:10.22331/q-2018-08-06-79.
- [17] Quantinuum. Quantinuum sets new record with highest ever quantum volume, September 2022. URL: <https://www.quantinuum.com/news/quantinuum-sets-new-record-with-highest-ever-quantum-volume>.
- [18] Nils Quetschlich, Lukas Burgholzer, and Robert Wille. MQT Bench: Benchmarking software and design automation tools for quantum computing. *Quantum*, 7:1062, July 2023. URL: <https://www.cda.cit.tum.de/mqtbench/>, [arXiv:2204.13719](#), doi:10.22331/q-2023-07-20-1062.
- [19] Seyon Sivarajah, Silas Dilkes, Alexander Cowtan, Will Simmons, Alec Edgington, and Ross Duncan. TKET: a retargetable compiler for NISQ devices. *Quantum Science and Technology*, 6(1):014003, November 2020. [arXiv:2003.10611](#), doi:10.1088/2058-9565/ab8e92.
- [20] Pauli Virtanen, Ralf Gommers, Travis E. Oliphant, Matt Haberland, Tyler Reddy, David Cournapeau, Evgeni Burovski, Pearu Peterson, Warren Weckesser, Jonathan Bright, Stefan J. van der Walt, Matthew Brett, Joshua Wilson, K. Jarrod Millman, Nikolay Mayorov, Andrew R. J. Nelson, Eric Jones, Robert Kern, Eric Larson, C. J. Carey, İlhan

Polat, Yu Feng, Eric W. Moore, Jake VanderPlas, Denis Laxalde, Josef Perkold, Robert Cimrman, Ian Henriksen, E. A. Quintero, Charles R. Harris, Anne M. Archibald, Antônio H. Ribeiro, Fabian Pedregosa, Paul van Mulbregt, Aditya Vijaykumar, Alessandro Pietro Bardelli, Alex Rothberg, Andreas Hilboll, Andreas Kloeckner, Anthony Scopatz, Antony Lee, Ariel Rokem, C. Nathan Woods, Chad Fulton, Charles Masson, Christian Häggström, Clark Fitzgerald, David A. Nicholson, David R. Hagen, Dmitrii V. Pasechnik, Emanuele Olivetti, Eric Martin, Eric Wieser, Fabrice Silva, Felix Lenders, Florian Wilhelm, G. Young, Gavin A. Price, Gert-Ludwig Ingold, Gregory E. Allen, Gregory R. Lee, Hervé Audren, Irvin Probst, Jörg P. Dietrich, Jacob Silterra, James T. Webber, Janko Slavič, Joel Nothman, Johannes Buchner, Johannes Kulick, Johannes L. Schönberger, José Vinicius de Miranda Cardoso, Joscha Reimer, Joseph Harrington, Juan Luis Cano Rodríguez, Juan Nunez-Iglesias, Justin Kuczynski, Kevin Tritz, Martin Thoma, Matthew Newville, Matthias Kümmerer, Maximilian Bolingbroke, Michael Tartre, Mikhail Pak, Nathaniel J. Smith, Nikolai Nowaczyk, Nikolay Shebanov, Oleksandr Pavlyk, Per A. Brodtkorb, Perry Lee, Robert T. McGibbon, Roman Feldbauer, Sam Lewis, Sam Tygier, Scott Sievert, Sebastiano Vigna, Stefan Peterson, Surhud More, Tadeusz Pudlik, Takuya Oshima, Thomas J. Pingel, Thomas P. Robitaille, Thomas Spura, Thouis R. Jones, Tim Cera, Tim Leslie, Tiziano Zito, Tom Krauss, Utkarsh Upadhyay, Yaroslav O. Halchenko, Yoshiki Vázquez-Baeza, and SciPy 1.0 Contributors. SciPy 1.0: fundamental algorithms for scientific computing in Python. *Nature Methods*, 17(3):261–272, Mar 2020. [arXiv:1907.10121](https://arxiv.org/abs/1907.10121), [doi:10.1038/s41592-019-0686-2](https://doi.org/10.1038/s41592-019-0686-2).

- [21] Finn Voichick, Leonidas Lampropoulos, and Robert Rand. COGNAC software, 2024. URL: <https://gitlab.umiacs.umd.edu/finn/cognac.git>.
- [22] Robert Wille, Rod Van Meter, and Yehuda Naveh. IBM’s Qiskit tool chain: Working with and developing for real quantum computers. In *2019 Design, Automation and Test in Europe Conference and Exhibition*, pages 1234–1240, New York, 2019. IEEE. [doi:10.23919/DATe.2019.8715261](https://doi.org/10.23919/DATe.2019.8715261).
- [23] Re-Bing Wu, Bing Chu, David H. Owens, and Herschel Rabitz. Data-driven gradient algorithm for high-precision quantum control. *Phys. Rev. A*, 97:042122, Apr 2018. [arXiv:1712.01780](https://arxiv.org/abs/1712.01780), [doi:10.1103/PhysRevA.97.042122](https://doi.org/10.1103/PhysRevA.97.042122).
- [24] Amanda Xu, Abtin Molavi, Lauren Pick, Swamit Tannu, and Aws Albarghouthi. Synthesizing quantum-circuit optimizers. *Proc. ACM Program. Lang.*, 7(PLDI), June 2023. [arXiv:2211.09691](https://arxiv.org/abs/2211.09691), [doi:10.1145/3591254](https://doi.org/10.1145/3591254).
- [25] Mingkuan Xu, Zikun Li, Oded Padon, Sina Lin, Jessica Pointing, Augustine Hirth, Henry Ma, Jens Palsberg, Alex Aiken, Umut A. Acar, and Zhihao Jia. Quartz: superoptimization of quantum circuits. In *Proceedings of the 43rd ACM SIGPLAN International Conference on Programming Language Design and Implementation, PLDI 2022*, page 625–640, New York, NY, USA, 2022. Association for Computing Machinery. [arXiv:2204.09033](https://arxiv.org/abs/2204.09033), [doi:10.1145/3519939.3523433](https://doi.org/10.1145/3519939.3523433).
- [26] Ciyu Zhu, Richard H. Byrd, Peihuang Lu, and Jorge Nocedal. Algorithm 778: L-BFGS-B: Fortran subroutines for large-scale bound-constrained optimization. *ACM Trans. Math. Softw.*, 23(4):550–560, December 1997. [doi:10.1145/279232.279236](https://doi.org/10.1145/279232.279236).
- [27] Zhiwen Zong, Zhenhai Sun, Zhangjingzi Dong, Chongxin Run, Liang Xiang, Ze Zhan, Qianlong Wang, Ying Fei, Yaozu Wu, Wenyan Jin, Cong Xiao, Zhilong Jia, Peng Duan, Jianlan Wu, Yi Yin, and Guoping Guo. Optimization of a controlled-z gate with data-driven gradient-ascent pulse engineering in a superconducting-qubit system. *Phys. Rev. Appl.*, 15:064005, June 2021. [arXiv:2104.11936](https://arxiv.org/abs/2104.11936), [doi:10.1103/PhysRevApplied.15.064005](https://doi.org/10.1103/PhysRevApplied.15.064005).

A Circuit depth metrics

Table 4 is similar to Table 1, except that it computes the circuit *depth*, counting only two-qubit gates.

Table 4. Two-qubit depth metrics from various optimizers

Benchmark	Optimized two-qubit circuit depth			
	Qiskit	TKET	Queso	COGNAC
ae	16	11	16	12
dj	3	3	3	3
ghz	3	3	3	3
graphstate	7	7	7	7
groundstate	20	19	20	17
grover-noancilla	69	52	69	24
grover-v-chain	69	52	69	24
portfolioqaoa	52	35	52	27
portfoliovqe	34	32	34	22
qaoa	12	9	15	10
qft	16	11	18	14
qftentangled	17	13	19	10
qnn	21	30	40	25
qpeexact	7	5	7	6
qpeinexact	13	10	14	14
qwalk-noancilla	163	157	163	30
random	36	32	37	30
realamprandom	34	32	34	27
su2random	34	32	34	23
tsp	11	11	11	6
twolocalrandom	34	32	34	27
vqe	5	5	5	5
wstate	5	5	5	5

B Alternative fidelity assumptions

Table 5 shows gate counts from the approximate optimizers when told that maximally entangling native two-qubit gates have 98% fidelity. Table 6 shows gate counts from the approximate optimizers when told that maximally entangling native two-qubit gates have 99.9% fidelity.

Table 5. Two-qubit gate counts, assuming 98% fidelity gates

Benchmark	Optimized two-qubit gate count		
	Qiskit	TKET	COGNAC
ae	11	11	14
dj	3	3	3
ghz	3	3	3
graphstate	8	8	8
groundstate	20	19	19
grover-noancilla	37	52	20
grover-v-chain	37	52	20
portfolioqaoa	40	35	20
portfoliovqe	34	32	18
qaoa	18	14	10
qft	8	11	11
qftentangled	13	13	9
qnn	21	21	19
qpeexact	8	6	6
qpeinexact	11	10	11
qwalk-noancilla	137	157	22
random	36	32	26
realamprandom	34	32	19
su2random	34	32	23
tsp	15	15	6
twolocalrandom	34	32	19
vqe	6	6	6
wstate	6	6	6

Table 6. Two-qubit gate counts, assuming 99.9% fidelity gates

Benchmark	Optimized two-qubit gate count		
	Qiskit	TKET	COGNAC
ae	16	11	12
dj	3	3	3
ghz	3	3	3
graphstate	8	8	8
groundstate	20	19	17
grover-noancilla	69	52	23
grover-v-chain	69	52	23
portfolioqaoa	52	35	31
portfoliovqe	34	32	28
qaoa	18	14	13
qft	18	12	13
qftentangled	19	14	12
qnn	40	31	29
qpeexact	8	6	6
qpeinexact	14	10	12
qwalk-noancilla	163	157	71
random	37	32	29
realamprandom	34	32	22
su2random	34	32	29
tsp	15	15	10
twolocalrandom	34	32	22
vqe	6	6	6
wstate	6	6	6